Evolution of microstructure in nanocrystalline Mo-Cu thin films during thermal annealing

G. Ramanath,[a] H. Z. Xiao, L. C. Yang, A. Rockett, and L. H. Allen
Coordinated Science Laboratory and Department of Materials Science and Engineering, University of Illinois at Urbana-Champaign, 1304 West Green Street, Urbana, Illinois 61801

(Received 6 March 1995; accepted for publication 10 April 1995)

The evolution of microstructure in Mo-Cu thin films during annealing has been investigated by *in situ* sheet resistance measurements, *ex situ* x-ray diffraction, and *in situ* hot-stage as well as conventional transmission electron microscopy. Mo-Cu thin films, deposited on various glass substrates by magnetron sputtering at ~30 °C, were supersaturated solid solutions of Cu in Mo with a nanocrystalline microstructure. The as-deposited films had large compressive residual stresses owing to the low homologous deposition temperature and low Ar pressure during deposition. Annealing results showed two distinct sets of microstructural changes occurring in the temperature ranges between ~300 and 500 °C, and ~525 and 810 °C. In the lower-temperature range, anisotropic growth of nanocrystallites was accompanied by stress relaxation without any observable phase separation. At temperatures greater than ~525 °C, the metastable solid solution collapsed and Cu precipitated at the grain boundaries. Increasing temperature resulted in the coarsening of Cu precipitates and simultaneous growth of Mo grains. At temperatures greater than ~700 °C, phase separation and grain growth approached completion. © *1995 American Institute of Physics.*

I. INTRODUCTION

Molybdenum is the ubiquitous choice for back contacts in solar cells based on copper indium diselenide ($CuInSe_2$, abbreviated as CIS) and related compounds.[1,2] Devices based on CIS have achieved conversion efficiencies exceeding 16%.[3–6] Device reliability is one of the major problems limiting large-scale production of CIS solar cells. Failures are commonly associated with a loss of adhesion at the CIS/Mo interface. Recently, it was found that the adhesion between the Mo back contact and the CIS absorber could be improved by using a contact metallization consisting of a metastable solid solution of Cu in Mo when the Cu content exceeded ~30 at.%.[7] During physical-vapor deposition of CIS on the Mo-Cu films at elevated temperatures, phase separation occurred in the back contact and Cu was released into the CIS layer. The release of Cu into the CIS film along with consequent changes in the microstructure and microchemistry of the back contact were apparently responsible for the improved adhesion. Also, photovoltaic devices based on CIS with Mo-Cu back contacts showed improved performance.[8] In this context, it is important to understand the microstructural changes taking place during annealing treatments.

This article presents the results of a study initiated to characterize the microstructural evolution of metastable Mo-Cu films during annealing to temperatures up to ~810 °C. Plausible mechanisms for observed microstructural changes are suggested and discussed in light of observations obtained from *in situ* sheet resistance, conventional transmission electron microscopy (TEM), *in situ* hot-stage TEM (HSTEM), and x-ray diffraction (XRD) analyses.

II. EXPERIMENTAL DETAILS

Mo-Cu films were deposited by magnetron sputtering in a four-chamber deposition system as described previously.[7,8] The films were sputtered onto thermally oxidized Si(100), Corning 7059 borosilicate glass, and soda-lime glass substrates. The dimensions of these substrates were typically $25\times25\times2$ mm^3. The Mo-Cu target was produced by attaching pieces of pure Cu foils to a Mo target. Different sizes of Cu strips were used to adjust the Cu content in the sputtered films. The films were sputtered in pure Ar at pressures ranging from 0.4 to 0.65 Pa (3–5 mTorr) at a sputtering current of 1 A maintained by a target voltage between 300 and 550 V. The substrates were unheated, resulting in a deposition temperature of ~25–35 °C. Film thicknesses of 200–2000 nm were obtained, at a deposition rate of ~50 nm/min. The results presented in this article are from experiments performed on Mo-Cu films sputtered on the thermally oxidized Si(100) substrates unless otherwise specified. Rutherford backscattering spectrometry using 2 MeV He^+ ions showed that these Mo-Cu films were ~200 nm thick, and had a Cu concentration of 30±2 at.%.

The samples were annealed in a vacuum furnace (base pressure 10^{-8} Torr) to temperatures up to ~810 °C at a ramp rate of 5 °C/min. The pressure during annealing was 1×10^{-7} Torr. The furnace is equipped with a four-point probe assembly for *in situ* sheet resistance measurements. Both the furnace and the four-point probe assembly are interfaced with a computer for control and data acquisition. Details of the experimental setup are reported elsewhere.[9] The temperature and the resistance of the samples were measured *in situ* during the anneals to monitor the changes occurring in the film. In the furnace annealing experiments the temperatures are estimated to be within ±20 °C. All temperatures reported in this article are rounded off to the nearest multiple of 5. The temperature coefficient of resistance (TCR) of the samples was measured between 30 and 200 °C after the various annealing treatments.

The annealed samples were characterized by XRD using a Rigaku D-Max III powder diffractometer using monochro-

[a]Electronic mail: ramanath@uiuc.edu

 0021-8979/95/78(4)/2435/6/$6.00

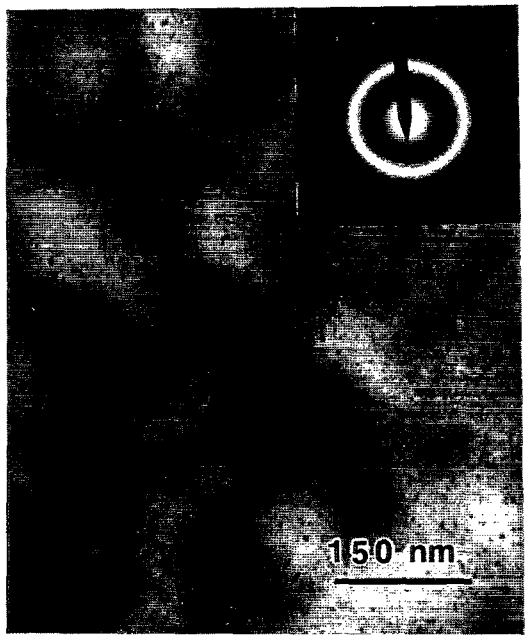

FIG. 1. Bright-field plan-view TEM micrograph showing the microstructure of the as-deposited Mo-Cu films. Nanocrystalline grains (<10 nm) are separated by regions of uniform contrast (10–15 nm). The selected-area-diffraction pattern (inset) shows broad rings associated with the bcc structure of a metastable Mo solid solution. The rings are indexed from the smallest to the largest as Mo(110), Mo(200), Mo(112), and Mo(220).

matic Cu K_α radiation. The intensity, linewidth, and the position of the x-ray peaks were determined from θ-2θ scans after aligning the diffractometer to the Si(400) peak. The position and the linewidth of the peaks were determined by fitting the peaks with Lorentzian curve fits. All the changes in the d spacings reported in this article are estimated to have a precision of ± 0.0005 nm. The full width half-maximum of the peaks was corrected for instrumental broadening by means of a standard Si sample.

Plan-view TEM studies were carried out using Philips 420 and CM12 TEMs, equipped with energy-dispersive x-ray detectors for local composition determination. TEM samples were prepared by dissolving the glass substrates in HF or by scraping the film off the glass using a razor blade. Films were then glued on 3 mm Cu grids and ion-milled on a cold stage (~77 K) using 5.0 keV Ar^+ ions. HSTEM analyses were performed in the Philips 420 TEM at temperatures between 20 and 800 °C.

III. RESULTS

Figure 1 shows that the as-deposited films consisted of nanocrystalline grains separated from each other by relatively large regions of uniform contrast. The diffraction pattern did not reveal any rings other than the broad rings associated with the bcc structure (see inset in Fig. 1), despite prolonged exposures (~300 s) of negatives in the TEM. XRD analyses of the as-deposited Mo-Cu films on the various glass substrates used in this study confirmed the electron

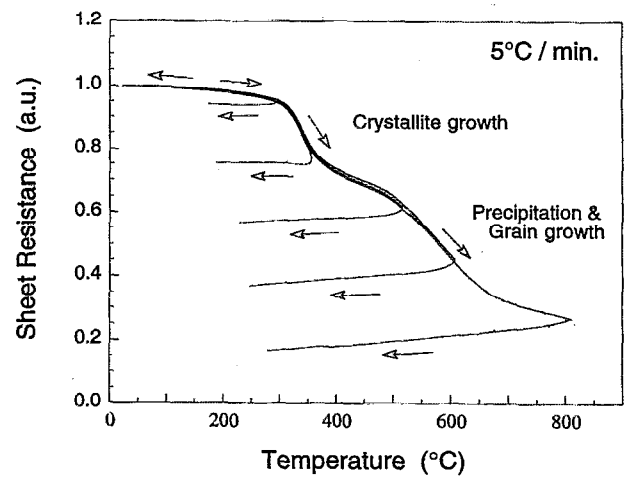

FIG. 2. Normalized sheet resistance vs temperature characteristics of Mo-Cu films, monitored *in situ* during annealing at a rate of 5 °C/min to various temperatures up to 810 °C. The arrows indicate the path followed by the resistance with increasing temperature. Samples annealed to different temperatures follow the same heating curve in the respective temperature ranges, indicating reproducibility.

diffraction observations that the as-deposited films consisted of a supersaturated (i.e., metastable) solid solution of Cu in Mo, irrespective of the glass substrate used.

Figure 2 shows *in situ* sheet resistance R normalized to that at 30 °C (6.6 Ω/□) vs temperature T curves obtained for the Mo-Cu films on thermally oxidized Si(100). For $T \lesssim 200$ °C, the R vs T curve was approximately linear and changes during heating were reversible during cooling. Between 300 and 500 °C, an irreversible 30% drop in the sheet resistance was observed, with most of the drop occurring between 300 and 400 °C. This correlated to microstructural changes occurring in the film, described below. For $T < 400$ °C, the R vs T behavior was the same for films on all substrates tested. The TCR of the as-deposited film was negative and had a value of −94 ppm/°C. The TCR of the films increased monotonically with annealing temperature as shown in Fig. 3. On annealing between 300 and 355 °C, the TCR became positive. Above 700 °C, the TCR approached the order of magnitude of the TCR of pure Mo (~5150 ppm/°C).

TEM analyses of samples annealed to temperatures less than 500 °C showed that the size of the nanocrystallites had increased (see Fig. 4). Electron diffraction revealed no observable phase separation processes in this temperature range (see inset in Fig. 4). Annealing of films that were removed from their substrates prior to the anneal yielded the same results. Figure 5 shows representative *ex situ* XRD results of films on thermally oxidized Si(100) annealed to various temperatures. It is evident that the intensity of the Mo(110) peak increased with annealing temperature. The Mo(112) XRD peak intensity also increased, but to a negligible extent. Films on other glass substrates also exhibited an increasing preference for the Mo(110) planes to be oriented parallel to the plane of the film during annealing. For example, on annealing to ~500 °C, films on slide glass showed a ~20% increase in Mo(110) peak intensity [normalized to the

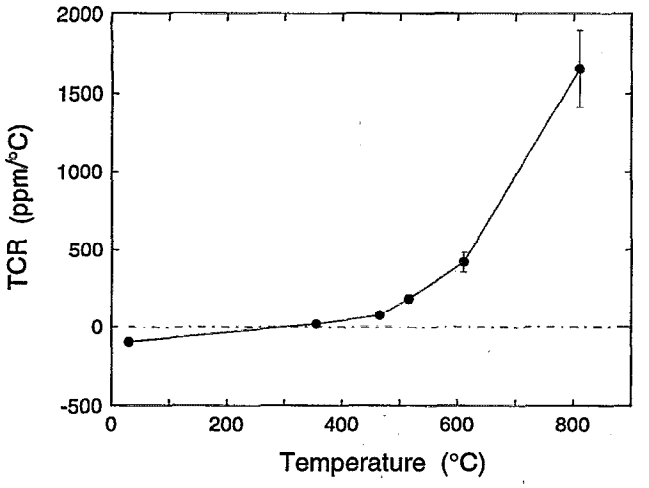

FIG. 3. Variation of the TCR of the films with annealing temperature. The TCR (normalized to 0 °C) was measured between 30 and 200 °C after the different annealing treatments (Ref. 11). Note the change in sign and magnitude of the TCR with increasing temperature of anneal.

Mo(112) peak]. While the initial texture of the film varied on different glass substrates, the Mo(110) texture enhancement on annealing appeared to be general, in the cases investigated.

The position and linewidth of the broad Mo(110) peak from the as-deposited sample are not apparent from Fig. 5. This is because the peak intensity, which is low against the background for the as-deposited sample, is plotted on a log scale. When the intensity was plotted on a linear scale, the position and the linewidth of the peak could be determined

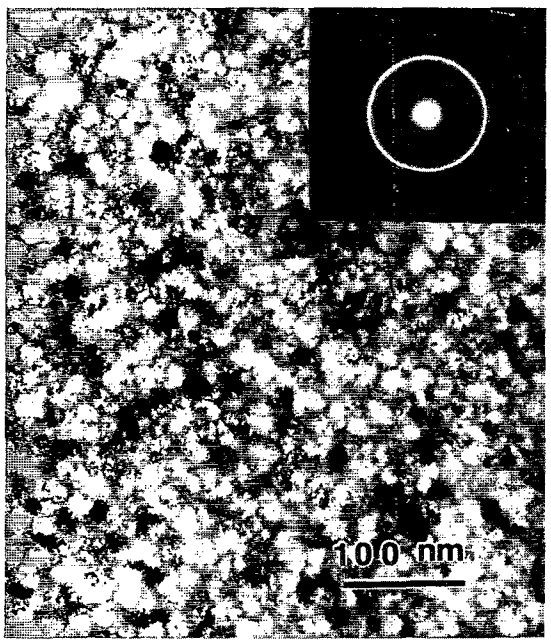

FIG. 4. *Ex situ* bright-field TEM micrograph of a sample annealed to 355 °C illustrates an increase in the average size of the nanocrystallites between 300 and 500 °C. The average grain size was between 27 and 35 nm. The selected-area-diffraction pattern in the inset shows the same rings as those in the as-deposited sample, indicating the absence of any noticeable phase separation phenomena in this temperature regime.

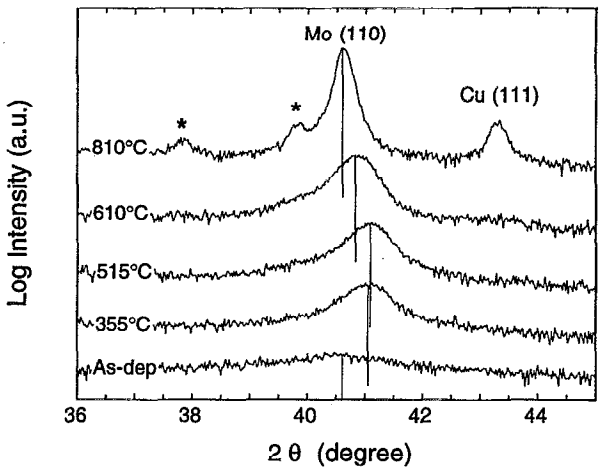

FIG. 5. Representative XRD results of Mo-Cu samples annealed to different temperatures at 5 °C/min. The curves are plotted on a log scale and are shifted vertically by arbitrary amounts for clarity. Note the increasing intensity, decreasing linewidth, and the shift in the peak position of the Mo(110) peak with increasing temperature. The approximate peak position is marked for each curve to facilitate visual comparison. The peaks marked * could not be indexed unambiguously.

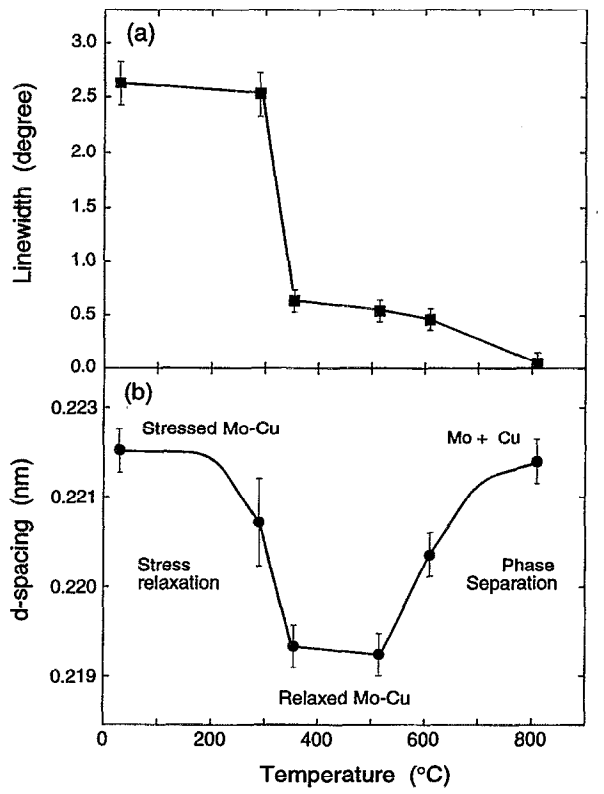

FIG. 6. Analyses of XRD results showing the variation of (a) the linewidth (full width at half-maximum) and (b) the d spacing (perpendicular to the plane of the film) associated with the Mo (110) XRD peak as a function of annealing temperature. The curve fit is drawn flat for temperatures below 200 °C as no irreversible changes occur in that regime. The processes related to the changes in the d spacing are indicated in the respective temperature regimes.

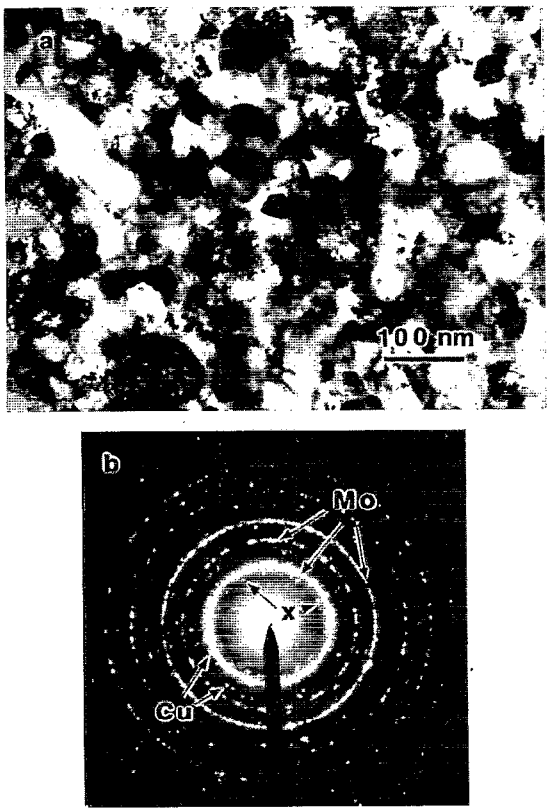

FIG. 7. (a) Bright-field TEM micrograph of a sample annealed to 810 °C at 5 °C/min shows coarsened Cu precipitates interspersed in a matrix of large Mo grains of sizes ranging between ~60 and 80 nm. (b) The selected-area-diffraction pattern reveals a two-phase mixture of bcc Mo and fcc Cu. Arrows indicate representative spots or rings associated with Mo(110), Mo(200), Mo(112), and Cu(111) and Cu(200) planes. Extra spots, for example, those marked ×, correspond to the extra peaks observed in the XRD pattern in Fig. 5.

unambiguously within acceptable error (see Fig. 6). Figures 6(a) and 6(b) illustrate the variation of the linewidth and the d spacing (perpendicular to the plane of the film) associated with the Mo(110) XRD peak as a function of annealing temperature. Note that the d spacing of (110) planes of the as-deposited Mo solid solution, perpendicular to the plane of the film, was the same as that of pure Mo (within experimental error). The large linewidth of the Mo(110) XRD peak in the as-deposited film is attributed to the small grain size. The decrease in the linewidth and the increase in the intensity of the Mo(110) peak were attributed to the increasing crystallite size for $T \leqslant 500$ °C.

Figure 2 shows a second irreversible resistance drop of ~60%, between 500 and 810 °C, with most of the change occurring below 700 °C. HSTEM showed that, at ~525 °C, the metastable nanocrystalline Mo-Cu solid solution collapsed with the onset of nucleation of fine-grained Cu precipitates. The coarsening of Cu precipitates was observed along with pronounced grain growth of the bcc Mo matrix, with increasing temperature. Precipitation and grain growth began to slow down at temperatures greater than ~700 °C, in agreement with the resistance results. TEM micrographs in Figs. 7(a) and 7(b) show the resulting microstructure of the sample annealed to 810 °C, and the corresponding selected-area-diffraction pattern, respectively. Energy-dispersive x-ray analysis of grains of various sizes showed that Cu grains were comparable in size with that of Mo grains. XRD analyses showed [see Fig. 6(b)] that the d spacing of the (110) planes increased and approached the value of that of pure Mo (0.222 nm), while the linewidth of the Mo(110) peak decreased simultaneously. The increase in the d spacing of (110) planes of Mo was correlated with the depleting Cu content in the solid solution. The decrease in the linewidth was attributed to the increasing size of the Mo grains. The Cu(111) XRD peak was clearly detectable after the anneal at 810 °C (see Fig. 5). The absence of any other Cu peaks indicated that the precipitation of Cu took place with a preferred orientation. XRD and electron-diffraction analyses of samples annealed to >600 °C revealed the emergence of extra spots and extra peaks respectively [see Figs. 5 and 7(b)]. These could not be indexed unambiguously. During HSTEM these diffraction spots were not observed and may have resulted from interactions of precipitated Cu with the SiO_2.[10]

IV. DISCUSSION

A. Crystallite growth and stress relaxation

The high sheet resistance and the low TCR of the as-deposited films were attributed to grain-boundary scattering due to the nanocrystalline microstructure, and impurity scattering resulting from the supersaturation of Cu in the Mo matrix.[11,12] The microstructure in the regions of uniform contrast in Fig. 1 is not discernible from our results. The uniform contrast may have resulted from nanocrystalline grains in those regions being oriented far away from the Bragg angle when imaged by bright-field TEM. Another possibility is that the regions of uniform contrast are amorphous. Considering the negative sign of the TCR, often observed in metallic alloys having high topological and structural disorder in microstructure,[13–15] it is likely that some of the regions between the nanocrystallites (i.e., the regions showing uniform contrast) are amorphous.

The reversible nature of the R vs T curve for $T \leqslant 200$ °C suggests that there are no appreciable microstructural changes occurring in the films in this temperature regime. The growth of the nanocrystallites occurring between 300 and 500 °C reduced the grain-boundary area and hence the grain-boundary scattering of electrons, causing the first drop in sheet resistance and the increase in TCR in this temperature regime. The enhancement of the (110) texture during growth indicates the preferential growth of grains with the (110) planes oriented parallel to the surface of the film, at the expense of the surrounding grains with unfavorable orientations and possibly amorphous regions.

The observed change in the (110) d spacing of the Mo solid solution, in the direction perpendicular to the plane of the film, can occur either due to a change in the impurity content in the solid solution or due to a change in the state of stresses in the film.[16] TEM and XRD results did not show any evidence of Cu precipitation for temperatures less than 515 °C, making the former possibility unlikely. It is also possible that the d spacing could change if gas atoms, trapped in

the film during deposition, escape from the film during annealing; however, for the deposition conditions used in our study, substantial gas trapping is not expected.[17,18] It has been shown that sputtering refractory metals at low homologous temperatures ($\lesssim 0.2T/T_m$) and low Ar pressures ($\lesssim$15 mTorr) results in compressive residual stresses.[18–20] Considering these factors, we propose that the observed change in the (110) d spacing of the Mo solid solution is caused by the relaxation of compressive residual stresses present in the Mo-Cu films due to the deposition conditions.

The fact that the (110) d spacing of the as-deposited Mo-Cu film was the same as that of pure Mo can be explained as a result of two opposing effects: Cu content and residual stress. Incorporation of Cu decreases the (110) d spacing of Mo, as is evident from the increase in d spacing accompanied by the precipitation of Cu between ~525 and 810 °C. The presence of uniform compressive residual stresses in the plane of the film causes an increase in the d spacing perpendicular to the plane of the film, owing to the Poisson effect.

Assuming the reduction in the Mo(110) d spacing below 515 °C to be entirely due to biaxial compressive residual stresses being relieved during annealing in this temperature range, the initial strain normal to the plane of the film in the as-deposited sample is ≈1.3%. If an elastic modulus of ≈320 GPa and a Poisson's ratio of 0.4 are associated with the film (these numbers are for Mo and its alloys[21]), the intrinsic biaxial residual compressive stress in the film would be of the order of ≈5 GPa. The extrinsic thermal stresses due to the coefficient of thermal-expansion mismatch between the substrate and the film[22] was estimated to be ≈0.3 GPa. The value of stress obtained is rather large when compared to the yield stress of typical metallic alloys (≈1 GPa); however, nanocrystalline microstructure can result in larger yield stresses.[13] Furthermore, stresses of ≈3.5 GPa have been reported in thin W films on SiO_2, sputtered at 370 °C and for thicknesses comparable to that of Mo-Cu films used in this study, under comparable deposition conditions.[20] The order of magnitude of the estimated stress is in the range of stresses developed in Mo (Ref. 19) and Cr films[19,20] sputtered at room temperature at low gas pressures.

As described earlier, annealing between 300 and 500 °C allowed anisotropic growth of crystallites in films on the original substrates, as well as in free-standing films (removed from their substrates). The principal difference between the two configurations is that, in the latter case, the free-standing films would have been able to curl up to relax the initially present residual stresses. The results indicate that the strain energy in the film due to residual stresses does not appear to play a significant role in the growth of the nanocrystallites. In that respect, the growth process is unlike the growth during strain energy driven recrystallization.[23,24]

Long-range transport of atoms would have led to Cu precipitation below 500 °C, which is contrary to our observations. Thus it is concluded that, below 500 °C, the growth of the nanocrystallites occurred by local shuffling of atoms at the grain boundaries. Near 400 °C, the insensitivity of resistance to temperature indicated that the crystallite growth process approached saturation, probably due to solute drag effects, i.e., the pinning of grain boundaries caused by the onset of segregation of Cu atoms to the grain boundaries.[25] It is interesting to find the growth of crystallites of a supersaturated solid solution without any observable phase separation, despite the large driving force for phase separation [Mo and Cu are immiscible at equilibrium for $T<900$ °C (Ref. 26)]. This may be suggestive of a high interfacial energy barrier for the formation of critical nuclei of Cu in these alloys; however, further understanding of the mechanisms of the processes occurring at these temperatures is required to explain this phenomenon.

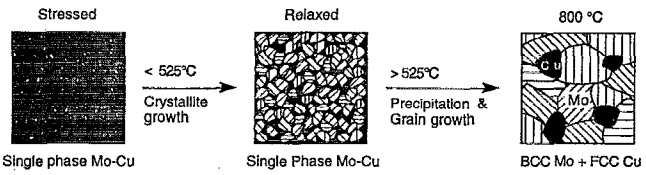

FIG. 8. A schematic view of the processes occurring during annealing of sputtered Mo-Cu films from room temperature to 810 °C. The dark background represents the microstructure of regions which may possibly be amorphous.

B. Phase separation and grain growth

Annealing to $T>525$ °C resulted in the precipitation of fcc Cu out of the solid solution. The high strain field arising from the large volume change associated with Cu precipitation (atomic volumes: Cu, 0.0118 nm^3/atom; Mo, 0.0156 nm^3/atom) and the small grain size of the Mo solid solution make Cu precipitation within the grains unfavorable. The lower cohesive energy of Cu (3.49 eV/atom) compared to Mo (6.82 eV/atom) favors Cu segregation to grain boundaries, where broken and distorted bonds are common, making intergranular precipitation most likely.[27] Therefore, it is inferred that the grain boundaries are the nucleation sites for the Cu precipitates, in agreement with previous results on Cu-Fe solid solutions.[28] The nucleation and growth of Cu precipitates has a high driving force and requires long-range transport of Cu atoms. The Cu atoms that pin the grain boundaries, towards the end of the stress relaxation process, diffuse along the grain boundaries to cluster and nucleate as precipitates. As the temperature rises, the rate of nucleation increases. The coarsening of the precipitates not only reduces their interfacial energy, but also decreases the number of pinning centers, thereby increasing the grain-boundary mobility.[25] This suggests that the grain growth observed at $T>525$ °C is driven by reduction in grain-boundary area and energy. Grain-boundary diffusion of Mo is the likely mechanism considering the temperature to be close to ≈0.3 T_m of Mo. Residual stresses, having been relieved at lower temperatures, had little influence above 525 °C. The decrease in sheet resistance and increase in TCR observed in the 525–700 °C temperature range apparently results from decreased grain-boundary scattering, decreased solute scattering and decreased local lattice distortion effects (due to Cu in the Mo solid solution),[11] and conduction through the resulting Cu grains. The various processes occurring during annealing are schematically represented in Fig. 8.

V. CONCLUSIONS

Microstructural evolution of sputtered Mo-Cu thin films on various glass substrates was investigated during thermal annealing. As-deposited films consisted of a metastable solid solution of Cu in Mo, with a nanocrystalline microstructure, and large compressive residual stresses. Between 300 and 500 °C anisotropic growth of the nanocrystallites occurred without long-range transport of atoms. The accompanying residual stress relaxation appeared to have little effect on the energetics of nanocrystallite growth. The crystallite growth process started to saturate near ~400 °C, probably because of solute drag effects. The changes observed below 500 °C were insensitive to the type of substrate used. At temperatures greater than ~525 °C, Cu precipitated out of the metastable solid solution at the grain boundaries. The coarsening of Cu precipitates was inferred to be the reason for the accompanying grain growth. Phase separation and grain growth saturated above 700 °C.

ACKNOWLEDGMENTS

H.Z.X., L.C.Y., and A.R. gratefully acknowledge the support of the Electric Power Research Institute (EPRI) under Contract No. RP-2702-1 and the National Renewable Energy Laboratory (Subcontract No. XAD-3-12114-1). G.R. and L.H.A. gratefully acknowledge support from the Petroleum Research Fund (ACS-PRF No. 25422-G5). G.R. would like to thank Professor Alwyn Eades and Professor Bob Averback (University of Illinois), and Dr. Cynthia Volkert (AT&T Bell Labs) for stimulating discussions during the course of this investigation. The authors would like to acknowledge the use of facilities at the Center for Microanalysis of Materials at the Materials Research Laboratory, University of Illinois, supported by the Department of Energy under Grant No. DEFG 02-91ER35439.

[1] J. Hedstrom, M. Bodegard, A. Kylner, L. Stolt, D. Hariskos, and H.-W. Schock, in *Proceedings of the 23rd IEEE Photovoltaic Specialists Conference*, Louisville, Kentucky, May 10–14 (IEEE, New York, 1993), p. 364.
[2] J. Ermer, R. Gay, D. Pier, and D. Tarrant, J. Vac. Sci. Technol. A **11**, 1888 (1993).
[3] A. Rockett and R. W. Birkmire, J. Appl. Phys. **70**, R81 (1991).
[4] W. E. Devaney and R. A. Mickelsen, Sol. Cells **24**, 19 (1988).
[5] R. W. Birkmire, L. C. Dinetta, P. G. Lasswell, J. D. Meakin, and J. E. Phillips, Sol. Cells **16**, 419 (1986).
[6] T. L. Chu, S. S. Chu, S. L. Lin, and J. Yue, J. Electrochem. Soc. **131**, 2182 (1984).
[7] L. C. Yang, L. J. Chou, A. Agarwal, and A. Rockett, in *Proceedings of the 22nd IEEE Photovoltaic Specialists Conference*, Las Vegas, October 7–11 (IEEE, New York, 1991), p. 1185.
[8] L. C. Yang and A. Rockett, J. Appl. Phys. **75**, 1185 (1994).
[9] L. H. Allen, Ph.D. thesis, Cornell University, 1990.
[10] J. Li, Y. S. Diamand, and J. W. Mayer, Mater. Sci. Rep. **9**, 1 (1992).
[11] J. K. Stanley, *Electrical and Magnetic Properties of Metals* (ASM, Metals Park, OH, 1963), p. 58.
[12] A. F. Mayadas and M. Shatzkes, Phys. Rev. B **1**, 1382 (1970).
[13] H. Gleiter, Prog. Mater. Sci. **33**, 223 (1989).
[14] J. H. Mooij, Phys. Status Solidi A **17**, 521 (1973).
[15] R. Zallen, *The Physics of Amorphous Solids* (Wiley, New York, 1983), p. 274.
[16] B. D. Cullity, *Elements of X-ray Diffraction*, 2nd ed. (Addison-Wesley, Reading, MA, 1978).
[17] B. Window, M. V. Swain, and G. L. Harding, Surf. Coat. Technol. **49**, 199 (1991).
[18] B. Window, G. L. Harding, C. Horrigan, and T. Bell, J. Vac. Sci. Technol. A **10**, 3278 (1992).
[19] J. A. Thornton and D. W. Hoffman, J. Vac. Sci. Technol. **14**, 164 (1977).
[20] R. C. Sun, T. C. Tisone, and P. D. Cruzan, J. Appl. Phys. **46**, 112 (1975).
[21] *Smithells Metals Reference Book*, 5th ed. (Butterworth, Washington, DC, 1976), 71st ed.
[22] Using data obtained from the *CRC Handbook of Chemistry and Physics*, edited by D. R. Lide (CRC, Boca Raton, FL, 1991).
[23] R. Venkatraman, J. C. Bravman, W. D. Nix, P. W. Davies, P. A. Flinn, and D. B. Fraser, J. Electron. Mater. **19**, 1231 (1990).
[24] R. W. Cahn, in *Physical Metallurgy*, edited by R. W. Cahn (Wiley, New York, 1965), p. 910.
[25] R. E. Reed Hill, *Physical Metallurgy Principles* (Litton, New York, 1973), p. 310.
[26] P. R. Subramanian and D. E. Laughlin, in *Binary Alloy Phase Diagrams*, 2nd ed., edited by T. B. Massalski (ASM International, Materials Park, OH, 1990), p. 1435.
[27] C. Kittel, *Introduction to Solid State Physics* (Wiley, New York, 1976), p. 74.
[28] J. Eckert, J. C. Holtzer, and W. L. Johnson, J. Appl. Phys. **73**, 131 (1993).